INSTRUCTIONS ON THE ANNOTATION OF PDF FILES

To view, print and annotate your article you will need Adobe Reader version 9 (or higher). This program is freely available for a whole series of platforms that include PC, Mac, and UNIX and can be downloaded from http://get.adobe.com/reader/. The exact system requirements are given at the Adobe site: http://www.adobe.com/products/reader/tech-specs.html.

Note: if you opt to annotate the file with software other than Adobe Reader then please also highlight the appropriate place in the PDF file.

<table>
<tr><th colspan="2">PDF ANNOTATIONS</th></tr>
<tr><th>Adobe Reader version 9</th><th>Adobe Reader version X and XI</th></tr>
<tr><td>When you open the PDF file using Adobe Reader, the Commenting tool bar should be displayed automatically; if not, click on ‘Tools’, select ‘Comment & Markup’, then click on ‘Show Comment & Markup tool bar’ (or ‘Show Commenting bar’ on the Mac). If these options are not available in your Adobe Reader menus then it is possible that your Adobe Acrobat version is lower than 9 or the PDF has not been prepared properly.
 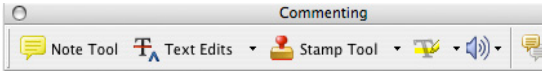

(Mac)
PDF ANNOTATIONS (Adobe Reader version 9)

The default for the Commenting tool bar is set to ‘off’ in version 9. To change this setting select ‘Edit | Preferences’, then ‘Documents’ (at left under ‘Categories’), then select the option ‘Never’ for ‘PDF/A View Mode’.
 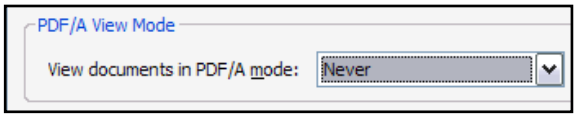

(Changing the default setting, Adobe version 9)</td><td>To make annotations in the PDF file, open the PDF file using Adobe Reader XI, click on ‘Comment’.

If this option is not available in your Adobe Reader menus then it is possible that your Adobe Acrobat version is lower than XI or the PDF has not been prepared properly.
 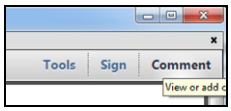

This opens a task pane and, below that, a list of all Comments in the text. These comments initially show all the changes made by our copyeditor to your file.
 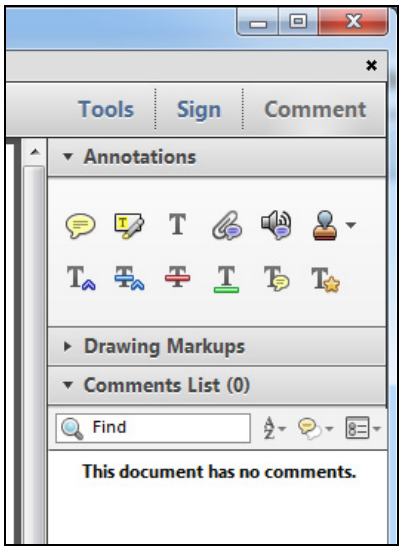
</td></tr>
</table>

HOW TO...		
Action	**Adobe Reader version 9**	**Adobe Reader version X and XI**
Insert text	Click the 'Text Edits' button on the Commenting tool bar. Click to set the cursor location in the text and simply start typing. The text will appear in a commenting box. You may also cut-and-paste text from another file into the commenting box. Close the box by clicking on 'x' in the top right-hand corner.	Click the 'Insert Text' icon on the Comment tool bar. Click to set the cursor location in the text and simply start typing. The text will appear in a commenting box. You may also cut-and-paste text from another file into the commenting box. Close the box by clicking on '_' in the top right-hand corner.
Replace text	Click the 'Text Edits' button on the Commenting tool bar. To highlight the text to be replaced, click and drag the cursor over the text. Then simply type in the replacement text. The replacement text will appear in a commenting box. You may also cut-and-paste text from another file into this box. To replace formatted text (an equation for example) please Attach a file (see below).	Click the 'Replace (Ins)' icon on the Comment tool bar. To highlight the text to be replaced, click and drag the cursor over the text. Then simply type in the replacement text. The replacement text will appear in a commenting box. You may also cut-and-paste text from another file into this box. To replace formatted text (an equation for example) please Attach a file (see below).
Remove text	Click the 'Text Edits' button on the Commenting tool bar. Click and drag over the text to be deleted. Then press the delete button on your keyboard. The text to be deleted will then be struck through.	Click the 'Strikethrough (Del)' icon on the Comment tool bar. Click and drag over the text to be deleted. Then press the delete button on your keyboard. The text to be deleted will then be struck through.
Highlight text/ make a comment	Click on the 'Highlight' button on the Commenting tool bar. Click and drag over the text. To make a comment, double click on the highlighted text and simply start typing.	Click on the 'Highlight Text' icon on the Comment tool bar. Click and drag over the text. To make a comment, double click on the highlighted text and simply start typing.
Attach a file	Click on the 'Attach a File' button on the Commenting tool bar. Click on the figure, table or formatted text to be replaced. A window will automatically open allowing you to attach the file. To make a comment, go to 'General' in the 'Properties' window, and then 'Description'. A graphic will appear in the PDF file indicating the insertion of a file.	Click on the 'Attach File' icon on the Comment tool bar. Click on the figure, table or formatted text to be replaced. A window will automatically open allowing you to attach the file. A graphic will appear indicating the insertion of a file.
Leave a note/ comment	Click on the 'Note Tool' button on the Commenting tool bar. Click to set the location of the note on the document and simply start typing. Do not use this feature to make text edits.	Click on the 'Add Sticky Note' icon on the Comment tool bar. Click to set the location of the note on the document and simply start typing. Do not use this feature to make text edits.

HOW TO...		
Action	**Adobe Reader version 9**	**Adobe Reader version X and XI**
Review	To review your changes, click on the 'Show' button 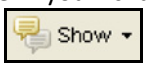 on the Commenting tool bar. Choose 'Show Comments List'. Navigate by clicking on a correction in the list. Alternatively, double click on any mark-up to open the commenting box.	Your changes will appear automatically in a list below the Comment tool bar. Navigate by clicking on a correction in the list. Alternatively, double click on any mark-up to open the commenting box.
Undo/delete change	To undo any changes made, use the right click button on your mouse (for PCs, Ctrl-Click for the Mac). Alternatively click on 'Edit' in the main Adobe menu and then 'Undo'. You can also delete edits using the right click (Ctrl-click on the Mac) and selecting 'Delete'.	To undo any changes made, use the right click button on your mouse (for PCs, Ctrl-Click for the Mac). Alternatively click on 'Edit' in the main Adobe menu and then 'Undo'. You can also delete edits using the right click (Ctrl-click on the Mac) and selecting 'Delete'.

SEND YOUR ANNOTATED PDF FILE BACK TO ELSEVIER

Save the annotations to your file and return as instructed by Elsevier. Before returning, please ensure you have answered any questions raised on the Query Form and that you have inserted all corrections: later inclusion of any subsequent corrections cannot be guaranteed.

FURTHER POINTS

- Any (grey) halftones (photographs, micrographs, etc.) are best viewed on screen, for which they are optimized, and your local printer may not be able to output the greys correctly.
- If the PDF files contain colour images, and if you do have a local colour printer available, then it will be likely that you will not be able to correctly reproduce the colours on it, as local variations can occur.
- If you print the PDF file attached, and notice some 'non-standard' output, please check if the problem is also present on screen. If the correct printer driver for your printer is not installed on your PC, the printed output will be distorted.

AUTHOR QUERY FORM

ELSEVIER	**Journal:** YARTH **Article Number:** 54976	**Please e-mail your responses and any corrections to:** **E-mail:** corrections.esi@elsevier.tnq.co.in

Dear Author,

Please check your proof carefully and mark all corrections at the appropriate place in the proof (e.g., by using on-screen annotation in the PDF file) or compile them in a separate list. Note: if you opt to annotate the file with software other than Adobe Reader then please also highlight the appropriate place in the PDF file. To ensure fast publication of your paper please return your corrections within 48 hours.

For correction or revision of any artwork, please consult http://www.elsevier.com/artworkinstructions.

Any queries or remarks that have arisen during the processing of your manuscript are listed below and highlighted by flags in the proof.

Location in article	Query / Remark: Click on the Q link to find the query's location in text Please insert your reply or correction at the corresponding line in the proof
	If there are any drug dosages in your article, please verify them and indicate that you have done so by initialing this query
Q1	Reference number mismatch in the sentence "Rehmer et al [4] showed that…" Kindly correct it.
Q2	Please define abbreviations "AX, AP, AR, AC, PC, and PR" in Figure 3 caption.
Q3	Please define abbreviations "AX, AP, AR, AC, PC, and PR" and "HN, NS0, NS8, and NS15" in figure captions 5, 6, and 7.
Q4	Please note that 5 or 6 keywords are mandatory as per journal style. Please provide appropriate number of keywords needed.
Q5	Please provide full-out first name for the author "O R" in reference 4.
Q6	Please provide full-out surname of the author "B C" in Reference 6.
Q7	Please confirm that given names and surnames have been identified correctly.
	Please check this box or indicate your approval if you have no corrections to make to the PDF file ☐

Thank you for your assistance.

The Journal of Arthroplasty xxx (2016) 1–5

Contents lists available at ScienceDirect

The Journal of Arthroplasty

journal homepage: www.arthroplastyjournal.org

Original article

The Effect of Impact Location on Force Transmission to the Modular Junctions of Dual-Taper Modular Hip Implants

Nicholas B. Frisch, MD, Jonathan R. Lynch, MD *, Richard F. Banglmaier, PhD, Craig D. Silverton, DO

Department of Orthopaedic Surgery, Henry Ford Health System, Royal Oak, Michigan

ARTICLE INFO

Article history:
Received 17 September 2015
Received in revised form
3 February 2016
Accepted 5 February 2016
Available online XXX

Keywords:
total hip arthroplasty
stability
modularity
corrosion

ABSTRACT

Background: The purpose of this study was to investigate the effect that off-axis impaction has on stability of dual-taper modular implants as measured by forces delivered to and transmitted through the head-neck and neck-stem tapers, respectively.

Methods: One hundred forty-four impact tests were performed using 6 different directions: one on-axis and five 10° off-axes. Four different simulations were performed measuring the head-neck only and 3 different neck angulations: 0°, 8°, and 15°. A drop tower impactor delivered both on- and off-axis impaction from a constant height. Load cells positioned in the drop mass and at the head-neck or neck-stem junction measured the impact and joint forces, respectively.

Results: Impact force of the hammer on the head ranged from 3800-4500 N. Greatest impact force delivered to the head was typically with axial impact. However, greatest force transmission to the neck-stem junction was not necessarily with axial impacts. There was limited variability in the force measured at the NS junction for all impaction directions seen in the 8° neck, whereas the 15° neck had greater forces transmitted to the NS junction with off-axes impactions directed in the proximal and posterior-proximal directions.

Conclusion: The location of the impact significantly influences the force transmitted to the head-neck and neck-stem junctions in dual-taper modular hip implants. Although axial impacts proved superior to off-axis impacts for the straight 0° neck, greater force transmission with off-axis impacts for the angled necks suggests that off-axis impacts may potentially compromise the stability of dual-taper components.

© 2016 Elsevier Inc. All rights reserved.

Mechanically assisted crevice corrosion is a wear-induced fretting corrosion of dual-taper modular total hip arthroplasty components. Relative component motion results in oxide layer abrasion and corrosion occurring at the interface between the head-neck (HN) or neck-stem (NS) junctions [1]. Risk factors exacerbating corrosion observed at these junctions are material combination, ball head diameter, neck length, and intraoperative assembly conditions [2]. The first 3 risk factors are implant design parameters, beyond the control of the surgeon. The last factor relates to the assembly of implant components within the operating theater. The ability to assemble the components becomes limited because of patient positioning and exposure of the components, with respect to the location of an applied impact seating force.

The debate continues in regard to the necessity of using hammer blows to assist the taper interaction at the HN and NS junctions to limit micromotion and subsequent corrosion. Pallini et al [3] concluded that hand assembly was sufficient because initial postoperative weight bearing would compress and seat the components. However, Mosley et al [4] concluded that fatigue performance of hand-assembled constructs were considerably less than that of hammer impact assembly because simulated gait loads produce off-axis loading. In addition, the ability to direct an ideal hammer blow along the axis of the mating components is exacerbated, as noted previously, by patient position and neck angulation. Effects of impact direction and neck angulation are not well studied.

One or more of the authors of this paper have disclosed potential or pertinent conflicts of interest, which may include receipt of payment, either direct or indirect, institutional support, or association with an entity in the biomedical field which may be perceived to have potential conflict of interest with this work. For full disclosure statements refer to http://dx.doi.org/10.1016/j.arth.2016.02.026.

* Reprint requests: Jonathan R. Lynch, MD, Department of Orthopaedic Surgery, Henry Ford Health System, 3107 Ferris Ave, Royal Oak, MI, 48073.

http://dx.doi.org/10.1016/j.arth.2016.02.026
0883-5403/© 2016 Elsevier Inc. All rights reserved.

UNCORRECTED PROOF

The purpose of this study was to evaluate the influence of impact location on the resultant forces transmitted to the HN and NS assembly joints for a variety of modular hip implant configurations. The ability to assemble the components becomes limited because of patient positioning, surgical exposure, and the requirement to apply a consistent axial force to the taper junction.

Methods

Dual hip implant assembly impacts were simulated to determine the resultant forces that would be transferred across the clinical implant mating taper joints between the HN and NS components. A total of 144 impact tests were performed simulating the assembly by impaction of the head onto the neck and the neck into the stem. Impacts consisted of those possible impacts directed both on and off axis to the longitudinal axis of the neck. For each component configuration tested, we mimicked 6 impact strikes: one directed along the axis of the neck or one of 5 separate off-axis strikes impacted 10° off the longitudinal axis of the neck.

Impact experiments used custom components fabricated to simulate modular implant components: the head and 0°, 8°, and 15° necks. The custom head was sized to a 32-mm implant head. The custom necks were manufactured to the measured length, width, and angle of their corresponding clinical implant necks. The custom head was attached to a post for measuring the force at the HN joint, or attached to one of the 3 custom necks for measuring the force at the NS joint (Fig. 1). The ends of the custom components matched the dimensions of the radiused elongated joint slot of the clinical stem but were not tapered. The joint slot was simulated by a load cell housing with a dimensionally matched radiused elongated slot without a taper. The components were inserted into this slot and rested on the load cell housed within to minimize relative motion between components. The untapered slot and component ends provided a snug slip fit to allow impingement on the load cell and unimpeded measurement of the simulated HN and NS joint forces directed along the axis of the slot depth, equivalent to the clinical implant taper axis (Fig. 2). Simulating the taper in the joint would have created an alternate load path around the load cell, decreasing the measurable force transmitted from the impact to the joint (We wanted to measure the force that would be available to engage the clinical implant components.) The simulated assemblies mimicking the HN and NS joints were designated as HN for the HN joint and NS0, NS8, or NS15 for the NS joints of the 0°, 8°, and 15° necks, respectively, or NS generally. Impacts to the simulated assemblies were delivered via a drop-mass impactor and impact tower representing the surgical hammer.

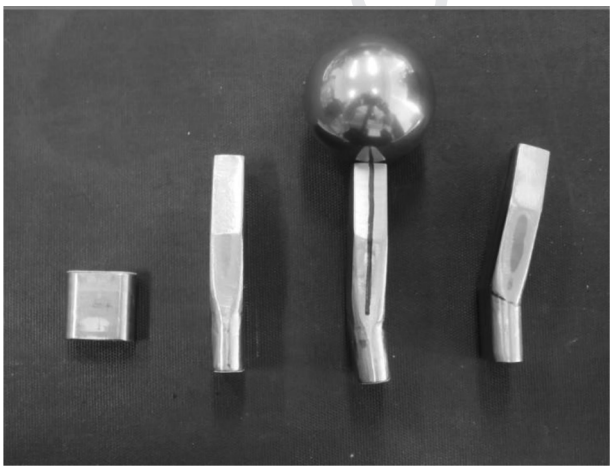

Fig. 1. Custom head and neck components. Moving from left to right, the post is depicted at the far left used for head-neck testing followed by 0° neck, 8° neck with the simulated head attached, and finally 15° neck at far right of the image.

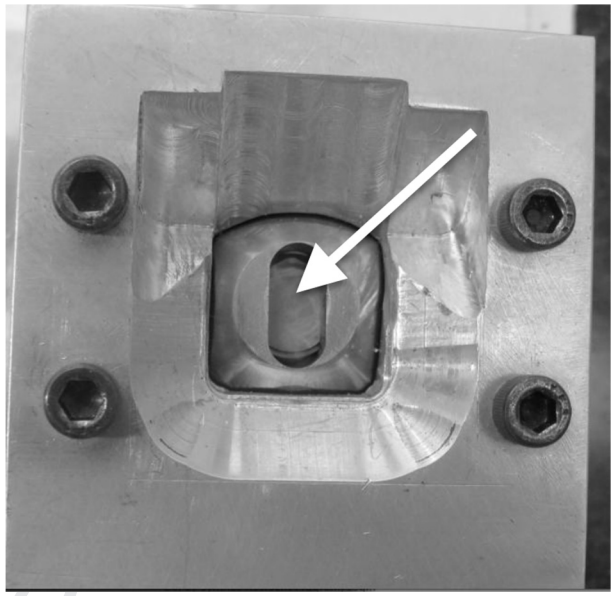

Fig. 2. View of the force measuring load cell (arrow) housed in the slotted load cell housing, which simulated the head-neck and neck-stem joints. The custom necks were inserted into this elongated slot and clamped using the top plate with 4 bolts. The simulated clinical joint slot could be rotated within the base fixture (not shown) to impart an off-axis impact located proximally (rotate toward top of the image), anteriorly (rotate toward right side of the image), or posteriorly (rotate toward left side of the image).

Impacts to the simulated assemblies were located at one of 6 positions on the custom head that represented possible impact strikes in the operating theater. These 6 impact locations were simulated by (1) axially directed along the long axis of the custom neck (AX); 10° from that axis in the (2) proximal (AP); (3) anterior (AR); or (4) posterior (PR) directions; and finally a combination of 10° off axis in the proximal direction with 10° in either the (5) anterior (AC); or (6) posterior (PC) directions (Fig. 3). Neck positions were adjusted to the desired impact location, clamped in place in the base fixture, and adjusted in the x-y direction to center the impact location on the head under the impactor.

A custom-built impact drop tower was used to guide the impactor onto the custom head of the simulated assemblies (Fig. 4). Preliminary tests were conducted to calibrate the drop height to the desired 4000-N impact force, which corresponded to a “firm” hammer blow delivered by the surgeon [5]. The impactor was raised to the calibrated height, held suspended by a switch activated magnetic clamp (Magswitch MagJig 60, MagSwitch Technology, Inc, Lafayette, CO), and then released. The impactor was directed onto the custom head via linear bearings and a guide rod attached to the impactor body. The impactor body was a steel mass, which allowed attachment of a load cell to record the impact forces delivered, and a Duralon load cell covering, which prevented sensor ringing from metal-to-metal impact.

Two load cells (Model 1051V6; Dytran Instruments, Inc, Chatsworth, CA) were used to measure the impact force delivered to the custom head of the simulated assembly and the resultant force measured at the slotted junction simulating either the HN or the NS joint. Both load cells were uniaxial. The load cell measuring the resultant HN or NS joint force only measured that force component directed along the axis of the slot’s depth. This force would be equivalent to the force that unites the clinical implant joint tapers.

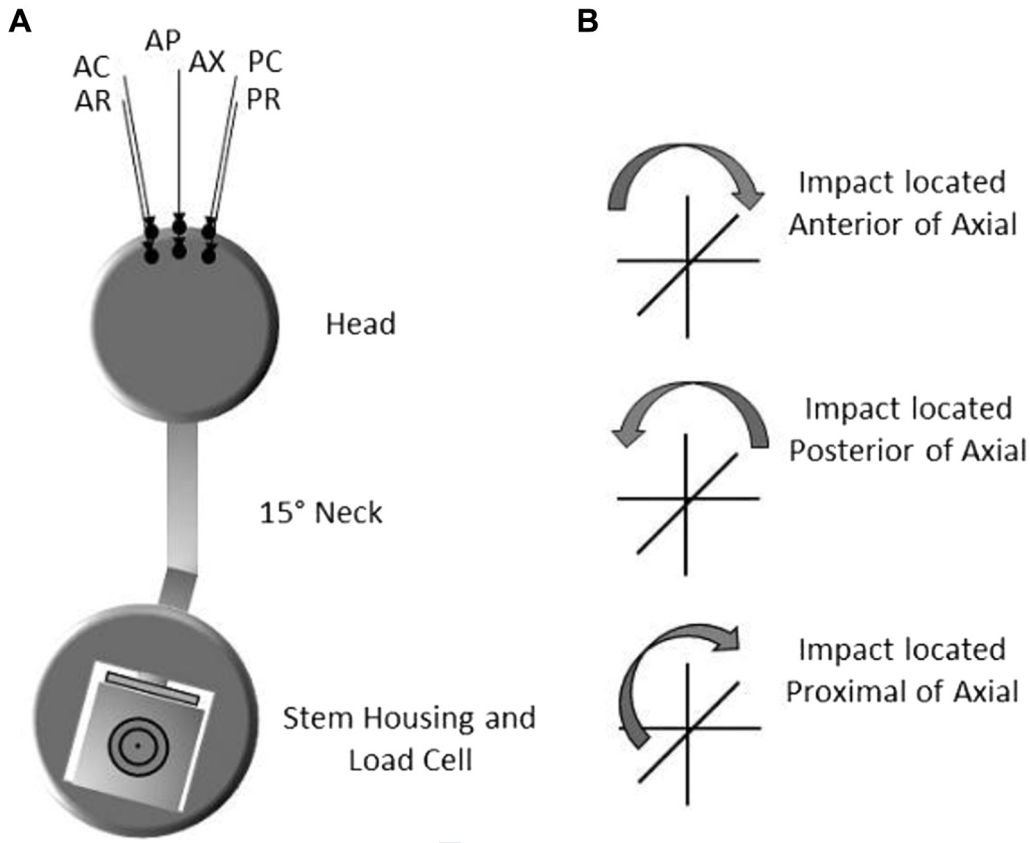

Fig. 3. Schematic of the impact locations (A) and rotations of the stem housing required to obtain proximal, anterior, or posterior impacts (B).

Impact and HN or NS joint forces measured with the 2 load cells were used to analyze differences among the simulated implant configurations. Off-axis impact and joint forces were compared to the commonly tested axial direction for the HN, NS0, NS8, and NS15. Joint forces were also compared for each of the 6 impact locations (AX, Pro AP, AR, AC, PC, PR). All comparisons used an analysis of variance test with the level of significance set to $\alpha = 0.05$.

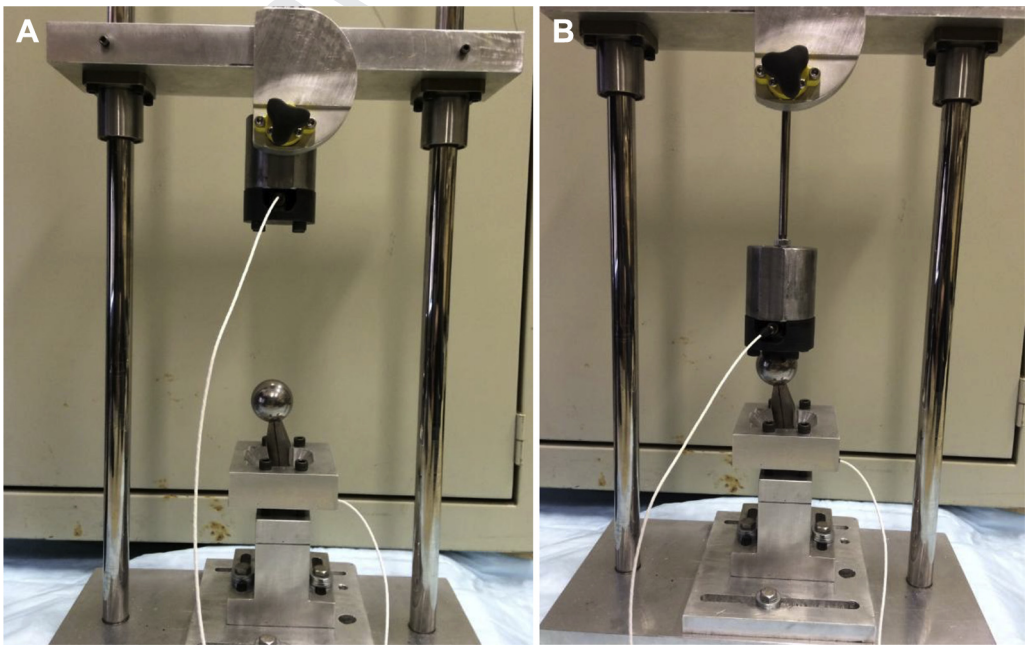

Fig. 4. Impact drop tower before (left) and after (right) impactor was dropped by releasing the magnetic clamp.

web 4C/FPO

Results

Simulated modular hip implant components were impacted using a linear drop mass. Preliminary calibration tests determined that a drop height of 141 mm imparted a 4000-N (standard deviation = ±99 N) impact force. This drop height was then used for the impact experiments to simulate the firm hammer blow of a surgeon [5]. This drop height was used across the spectrum of head and neck impact locations to maintain a consistent and representative surgical hammer blow for all 144 experiments.

Impact force measurements showed that the firm hammer blow imparted forces that changed with the impact location, ranging from approximately 3800-4500 N. Generally, the impact forces followed the trend that AX-directed impacts resulting in the highest forces followed in a decreasing order by the AP impacts, AR or PR impacts, then the combined AC or PC impacts with the AC and PC impact forces typically the lowest (Fig. 5). Impact forces measured in the HN were consistent with those delivered to NS0, NS8, and NS15. Within each simulated joint, the impact forces measured for the commonly tested AX location were most often significantly higher than those in the AR, AC, PC, and PR locations but not the AP impacts. The impact forces for the AX location were also not different from the AC and PR locations in the HN and the PR location in the NS8. An exception was found for the AR location in the HN, which resulted in significantly higher forces than the AX impact forces.

Forces measured at the HN or NS joint exhibited some similarity to the impact force trends, as described previously, but the differences between the AR, AC, PC, and PR locations were attenuated within the NS0 and NS8 series of impacts (Fig. 6). While the joint forces ranged from approximately 3900-4500 N, only the PR impact in the NS0 was significantly lower than the AX impact location. The exception to these observations was NS15 which did not follow the impact force trend nor result in attenuated joint forces. Within this group of experiments, the joint forces ranged from approximately 3800-5000 N and the AP, AC, and PC locations exhibited joint forces above the AX location. The AP joint force was significantly greater than the AX by 855 N.

Looking at the joint forces at each impact location, we see that the forces transmitted across the HN would not vary significantly compared to NS0 and NS8 for most locations (Fig. 7). Except for the AR location, the HN forces were not significantly different than those measured at NS0 and NS8. AR impacts resulted in joint forces at HN that were significantly higher than at NS0, NS8, and NS15. Overall, the joint forces of NS15 behaved much differently than the other necks. AX-located impacts showed that the NS joint forces decreased with increased neck angle where NS15 had significantly lower forces than NS0 and HN. The AR and PR impact locations also showed decreased forces for NS15, yet only significantly lower than HN for the PR impact. On the contrary, the NS joint forces of NS15 were significantly greater than all others in the AP location. The PC location impacts also resulted in a significant increase in the joint forces of NS15 compared to NS8 and HN.

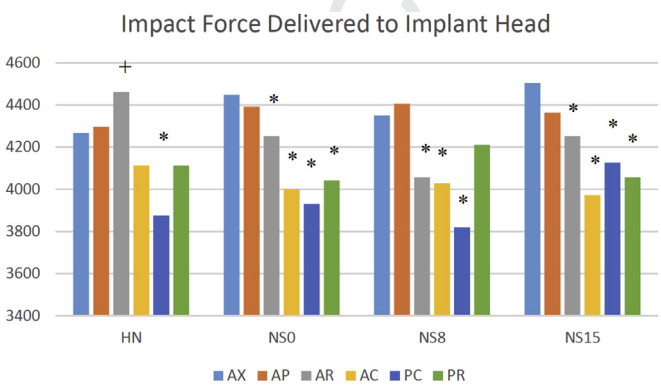

Fig. 5. Resultant impact forces delivered to the custom head, which simulated the implant head.

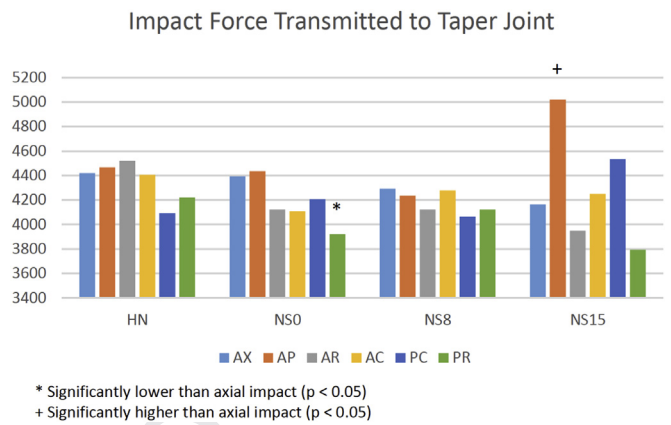

Fig. 6. Resultant impact forces delivered to the simulated neck-stem taper. Comparisons are within each simulated head or neck system.

Discussion

It is well understood that cyclic loading induces the causal micromotion mechanism of fretting corrosion. Routine physical activities such as walking in the immediate postoperative period generate forces that well exceed the minimal force required to generate fretting and corrosion. In vitro studies have demonstrated that fretting currents are strongest in the first 10,000-1,000,000 cycles [6-8]. With the average patient walking 2 million gait cycles a year [9], this correlates with in vivo retrieval studies identifying significant fretting corrosion of the NS taper as soon as 17 months postoperatively [10]. Proper component seating and engagement of the clinical implant mating tapered joints is generally accepted as the mitigating factor improving stability of those joints. However, the method of achieving stable engagement is still debated. Manual assembly followed by patient weight mobilization and weight

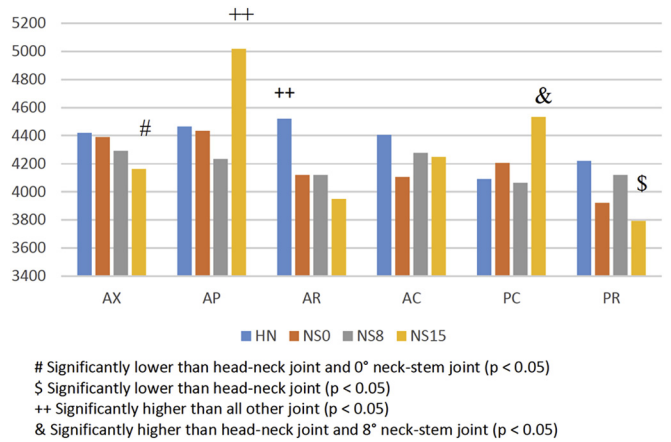

Fig. 7. Resultant impact forces delivered to the simulated neck-stem taper. Comparisons are between each simulated head or neck system.

web 4C/FPO
Q3
CORRECTED PROOF

bearing [3] and hammer blow [4,5] are the two competing methods to achieve implant stability.

Concern for the use of these assembly methods arises from less-than-ideal assembly scenarios. For instance, weight bearing and gait loads are applied off axis [11], and physical constraints in the operating theater may prevent axial hammer impaction. Prior studies investigated the ideal conditions of axial impact blows or axial monotonic compression (simulating body weight) to engage the clinical implant mating tapered surfaces [3,5]. Therefore, this study investigated the consequences of off-axis loading.

Pallini et al [3] showed that the disassembly force required to disassemble the NS taper with the combination of manual insertion followed by the simulated postoperative gait loads was as high as that obtained with simulated hammer blows. Although this may lead to a stable taper junction following several rounds of an ideally axially directed experimental cyclic loading, concern with this approach would be the in vivo micromotion and potential for fretting corrosion at the joint due to off-axis gait loads. In their study, simulated gait loads were directed axially along the neck axis of a 0° neck, whereas joint reaction forces at the hip [11] would not be aligned with the axis of the taper in clinical implants. Therefore, the resultant moment acting on the taper would not unite the components as in their study. The decreased NS force of off-axis impacts in the 0° neck observed in the present study may be clinically relevant and better explains the force transmission for such hand assembly and gait loaded implants. Force vectors acting off the axis of the taper not only effect seating of the components but have been suggested to be a potential initiator of fretting at the time of surgery [9]. Although only the PR-directed impacts for the NS0 transmitted significantly lower forces to the NS joint, this study only investigated impacts as far as 10° off the axis of the neck and impacts made at greater angles would be expected to reach statistical significance.

Rehmer et al [4] showed that the impact force was positively correlated with the implant stability, measured by the force required to separate the mating taper joint, for axial impacts. On the other hand, we found that the impact force was significantly affected by the location of the impact for a given neck while maintaining a consistent firm hammer blow. Axial impacts and those offset 10° proximally were not significantly different, yet those impacts offset 10° anteriorly, posteriorly, or a combined anteroproximal or posteroproximal were less than the ideal axial impact. This trend was consistent among the different neck angulations.

Mitigating these observed effects of impact location on impact force was the attenuation of differences between those forces as they were transmitted to the NS. However, the axial, anterior, and posterior impact directions showed that the increasing neck angle was associated with decreasing NS taper joint forces, which could affect seating, as noted previously. The suspected reason for these decreased joint forces is due to greater impingement and binding of the neck in the elongated stem slot due to of the introduction of rotation moments from the off-axis force, especially for the anterior and posterior impact locations. Mechanically, the angulated necks result in an applied moment, which increases the reaction force between the slot surface and the neck. The reaction forces are normal to the elongated slot surface, which increases the friction forces. Proximal impacts alleviate the binding because the reaction forces are applied to a smaller surface area in the radiused ends of the elongated slot, which reduced the normal forces acting on the components.

Introducing a bend in the neck for the 8° and 15° necks means that the HN and NS tapers are no longer in line with one another. Attempting to impact a dual-taper, angled-neck component with a single impaction means that the impact delivered will be off the longitudinal axis of at least one, if not both, of the tapers. This is shown in the forces measured at the NS taper for the angled necks as the axial impacts do not prove to be superior to some of the off-axis impacts as described previously. Thus, although the axial impacts were in line with the HN taper axis, they were not in line with the NS taper axis which explains the attenuation in forces. With an angle in the neck, the question becomes what impact direction will improve the stability of both the HN and NS tapers? Impaction results suggest that axial or proximal impacts are preferred for lower-angle necks, whereas proximal or combined posteroproximal impacts are preferred in high-angle necks. The increased forces transmitted to the NS with preferred impacts would be expected to lead to more stable components in clinical implants.

In conclusion, the direction at which dual-taper modular implants are impacted at index surgery does appear to have a significant effect on the forces transmitted to the modular taper interface. Although axial impaction appears ideal for a straight neck, the ideal direction of impaction for an angled neck appears to be dependent on the magnitude of the neck angle. The results of our study suggest that axial or proximal impacts are preferred for 0° and 8° necks, whereas proximal or posterior proximal impacts are preferred for 15° necks. As a result of this study, it is clear that the ability to have a consistent stable modular junction with dual-taper components is affected by the direction of the impacted force. The operating surgeon has limited control of this process. Adding another taper junction to standard total hip replacements has negated the benefits afforded by modularity and created new and previously unreported complications of corrosion and neck fractures [8]. However, understanding the mechanism by which these complications and failures occur may provide us with more insight in the future in the designing of newer implants.

Acknowledgments

The authors thank Dr Yener Yeni for allowing them to conduct this biomechanical study in his machining and testing laboratory.

References

1. Hariri S, Safran MR. Ulnar collateral ligament injury in the overhead athlete. Clin Sports Med 2010;29(4):619.
2. Srinivasan A, Jung E, Levine BR. Modularity of the femoral component in total hip arthroplasty. J Am Acad Orthop Surg 2012;20(4):214.
3. Pallini F, Cristofolini L, Traina F, et al. Modular hip stems: determination of disassembly force of a neck-stem coupling. Artif Organs 2007;31(2):166.
4. Mosley J, O R, Roark M, et al. Accelerated fretting corrosion testing of modular necks for THA. In: ORS 2013 Annual Meeting: Wright Medical Technology; 2013. n/a.
5. Rehmer A, Bishop NE, Morlock MM. Influence of assembly procedure and material combination on the strength of the taper connection at the head-neck junction of modular hip endoprostheses. Clin Biomech (Bristol, Avon) 2012;27(1):77.
6. Goldberg JR, B C, Jacogs JJ, et al. *Corrosion testing of modular hip implants*. West Conshohocken, PA: Americal Society of Testing Materials; 1997.
7. Nganbe M, Khan U, Louati H, et al. In vitro assessment of strength, fatigue durability, and disassembly of Ti6Al4V and CoCr Mo necks in modular total hip replacements. J Biomed Mater Res B 2011;97B(1):132.
8. Nganbe M, Louati H, Khan U, et al. Retrieval analysis and in vitro assessment of strength, durability and distraction of modular total hip replacement. J Biomed Mater Res A 2010;95A(3):819.
9. Silva M, Shepherd EF, Jackson WO, et al. Average patient walking activity approaches 2 million cycles per year: pedometers under-record walking activity. J Arthroplasty 2002;17(6):693.
10. Kop AM, Swarts E. Corrosion of a hip stem with a modular neck taper junction: a retrieval study of 16 cases. J Arthroplasty 2009;24(7):1019.
11. Keyak JH, Skinner HB, Fleming JA. Effect of force direction on femoral fracture load for two types of loading conditions. J Orthop Res 2001;19(4):539.

UNCORRECTED PROOF